International Journal of Design & Nature and Ecodynamics
Vol. 20, No. 12, December, 2025, pp. 2883-2896
Journal homepage: http://iieta.org/journals/ijdne

A Novel SNEDDS Formulation of *Swietenia mahagoni Jacq* and *Peperomia pellucida* L: Antidiabetic Potential and Molecular Docking Insights

Hartati Hartati[1*], Hartono Hartono[1], Suriati Eka Putri[2], Rizal Irfandi[2], Satria Putra Jaya Negara[2], Fastabiqul Khaeratih[3], Sahribulan Sahribulan[1]

[1] Department of Biology, Universitas Negeri Makassar, Makassar 90224, Indonesia
[2] Department of Chemistry, Universitas Negeri Makassar, Makassar 90224, Indonesia
[3] Postgraduate Student of Biotechnology, Universitas Negeri Makassar, Makassar 90224, Indonesia

Corresponding Author Email: hartati@unm.ac.id

https://doi.org/10.18280/ijdne.201213

Received: 15 November 2025
Revised: 17 December 2025
Accepted: 24 December 2025
Available online: 31 December 2025

Keywords:
antidiabetic, Swietenia mahagoni, Peperomia pellucida, SNEDDS, GC–MS, molecular docking

ABSTRACT

The present study aims to develop and characterize a Self-Nanoemulsifying Drug Delivery System (SNEDDS) formulation containing a combination of *Swietenia mahagoni* Jacq. (mahogany) seed extract and *Peperomia pellucida* L. (pepper elder) leaf extract as a potential antidiabetic therapy. Physicochemical characterization demonstrated that the best SNEDDS possessed a homogeneous globule size distribution (11.29 ± 0.88 nm), a zeta potential of –10.33 mV, and a polydispersity index (PDI) value of 0.35 ± 0.29, indicating excellent stability and uniformity of the nanoemulsion system. Gas Chromatography–Mass Spectrometry (GC–MS) analysis identified four major fatty acid methyl esters, namely methyl oleate (61.17%), methyl palmitate (8.07%), methyl stearate (6.20%), and methyl linoleate (6.48%), demonstrating that the oil phase was rich in monounsaturated fatty acids (MUFA), particularly oleic acid. These bioactive lipids contribute to enhanced insulin sensitivity and reduced inflammation, supporting the antidiabetic mechanism of the formulation. In vivo studies in diabetic rats showed that SNEDDS formulation significantly reduced blood glucose levels, with the highest reduction observed in the SMSC1A (FB 1:1) group, showing a glucose-lowering effect of up to approximately 82% compared to post-induction levels. Molecular docking analysis using the free fatty acid form (9-octadecenoic acid) against protein tyrosine phosphatase 1B (PTP1B) provided supportive mechanistic insight into the potential role of unsaturated fatty acids in modulating insulin signaling. Overall, the results indicate that the developed SNEDDS enhances the delivery of bioactive phytoconstituents and exhibits promising antidiabetic potential.

1. INTRODUCTION

The utilization of herbal plants as sources of natural therapeutics continues to be widely accepted, as they are generally associated with fewer adverse effects compared to synthetic pharmaceuticals. Herbal-based treatments are predominantly formulated in oral dosage forms due to their favorable safety profile, ease of administration, and cost-effectiveness [1]. However, low solubility and poor oral bioavailability reduce the effectiveness of the drugs in the body. Therefore, it is necessary to develop nanoemulsion drug formulations that can increase the bioavailability and solubility of drugs from herbal plant extracts. One such system is the Nanoemulsion Drug Delivery System (NEDDS) [2]. This technological utilization system utilizes nanotechnology, which provides a synergistic platform for developing potent antibacterial agents with enhanced therapeutic performance [3].

NEDDS represents a lipid-based delivery system designed to improve the solubility and bioavailability of hydrophobic pharmaceuticals and bioactive food constituents. This system comprises an isotropic blend of oils, surfactants, cosurfactants, and bioactive compounds that, upon dispersion in an aqueous medium, can spontaneously generate oil-in-water nanoemulsions within the gastrointestinal tract, producing droplets on the nanometer scale [4]. NEDDS have many advantages, including maximizing drug absorption and transport, modulating drug biodistribution and disposition, and delivering drugs to targets, thereby reducing side effects. Compared to other nanoemulsion systems, NEDDS formulations tend to be more physically and chemically stable for long-term storage [5]. This study used Box Behnken Design to optimize NEDDS from mahogany seed extract using Design Expert 8.0.5 (State-Ease Inc., Minneapolis, USA) computer programming.

It has been previously observed that Self-Nanoemulsifying Drug Delivery System (SNEDDS) from various plant extracts have antidiabetic properties. Biochemical, hematological, and histological evaluations in streptozotocin-induced diabetic rats indicate that the SNEDDS formulation derived from ripe *Momordica charantia* fruit, with a particle size of 31.89 nm, exhibits substantial potential as an antidiabetic agent [6].

Additionally, when curcumin extract is added to the SNEDDS recipe, the therapeutic effect on diabetes mellitus is improved [7]. It demonstrates that adding two different kinds of plant extracts to the SNEDDS mix can increase its antidiabetic effectiveness.

In Indonesia, *Swietenia mahagoni* (mahogany) seeds are widely used in traditional medicine for hypertension, diabetes, malaria, and wound healing. Furthermore, the seeds have therapeutic effects due to the presence of biologically active compounds, such as fatty acids and tetranortriterpenoids. Mahogany seeds have antimicrobial, anti-inflammatory, hepatoprotective, antidiarrheal, antiulcer, depressant, anticonvulsant, and neuropharmacological activities, as well as antidiabetic, anti-HIV, immunomodulatory, antifungal, antioxidant, analgesic, platelet aggregation inhibitor, antimutagenic, and anticancer properties [8]. Mahogany seed oil extract is excellent for developing nanoemulsions. *Peperomia pellucida* L. Kunth (*Familia Piperaceae*) is a traditional medicinal plant used to treat various types of diseases. This plant promises to be a potential source of new drugs for various diseases, having anti-inflammatory, antimicrobial, antioxidant, anticancer, and antidiabetic activities.

Therefore, the development of lipid-based nanoemulsion systems such as SNEDDS represents a promising strategy to enhance the oral delivery and therapeutic performance of plant-derived bioactive compounds. The selection of *Swietenia mahagoni* and *Peperomia pellucida* for combination in an SNEDDS formulation was based on their complementary traditional usage and phytochemical characteristics, rather than on previously established pharmacological synergy. *Swietenia mahagoni* seeds have been extensively used in traditional medicine for the management of diabetes mellitus and are known to contain lipophilic bioactive compounds, including fatty acids and limonoids, which exhibit antidiabetic, anti-inflammatory, and insulin-sensitizing activities [8, 9]. These lipophilic constituents are particularly suitable for incorporation into lipid-based delivery systems such as SNEDDS, which are designed to enhance the solubility and oral bioavailability of poorly water-soluble compounds [4, 5].

In contrast, *Peperomia pellucida* leaves are traditionally used to treat metabolic and inflammatory disorders and have been reported to contain polar and semi-polar phytochemicals, such as flavonoids, phenolics, alkaloids, and amide compounds, which contribute to antidiabetic and antioxidant activities through mechanisms distinct from lipid-based constituents [10, 11]. The combination of these two plant extracts was therefore hypothesized to provide a broader spectrum of antidiabetic bioactivity by integrating lipophilic and more polar phytoconstituents within a single SNEDDS platform.

This formulation strategy was intended to enhance the delivery and biological performance of diverse phytochemicals rather than to assert a confirmed synergistic pharmacological effect. The potential synergistic or additive interactions between the extracts remain an important subject for future investigation. To the best of the authors' knowledge, no prior research has examined the use of extracts from mahogany seeds and *Peperomia pellucida* L. leaves in SNEDDS antidiabetic medication compositions. In order to produce a supply of raw materials to combat diabetes in the form of SNEDDS, this study synthesized a blend of *Swietenia mahagoni* seed extract and *Peperomia pellucida* L. leaf extract.

2. MATERIALS AND METHOD

2.1 Materials

The materials employed in this study included mahogany seeds, pepper elder, ethyl acetate, 96% ethanol, Tween 80, PEG 400, aquabidest, distilled water, filter paper, alloxan, glibenclamide, aluminum foil, male *Mus musculus* mice, Na-CMC, a 5% glucose solution, and glucose test strips.

2.2 Sample preparation and extraction of mahogany seeds

In this research, two types of plants, namely mahogany seeds and pepper elder, were studied. Sample preparation and extraction were carried out as follows: Mahogany seed samples were separated from the seed coat and cleaned, then cut into pieces and dried. After drying, the mahogany seed samples were ground. The illustration of sample preparation is shown in Figure 1.

Extraction was performed using the Soxhlet technique with ethyl acetate as the solvent. A 5-g portion of mahogany seed powder was loaded into a 25 mm × 100 mm thimble chamber, and 150 mL of ethyl acetate was placed in the flask. The extraction proceeded for 6 hours at 65°C, after which the filtrate was concentrated using a rotary evaporator to obtain a viscous extract, which was subsequently stored until further use. Pepper elder leaves were washed, dried, and then pulverized. A total of 150 g of the resulting leaf powder was macerated with 482 mL of 70% ethanol for 24 hours, combining the extract from three successive maceration cycles.

Next, the filtrate was evaporated using a rotary evaporator to obtain a thick extract and stored until used. *Peperomia pellucida* L. leaves were cleaned and dried, then ground. *Peperomia pellucida* L. leaves that had been ground in powder form were weighed at 150 g, then macerated with 482 mL of 70% ethanol for 24 hours (combined from 3× extractions). Next, the filtrate was evaporated using a rotary evaporator. The results of the evaporated extract obtained a thick extract and stored until used for further analysis. The illustration of the extraction process is shown in Figure 2.

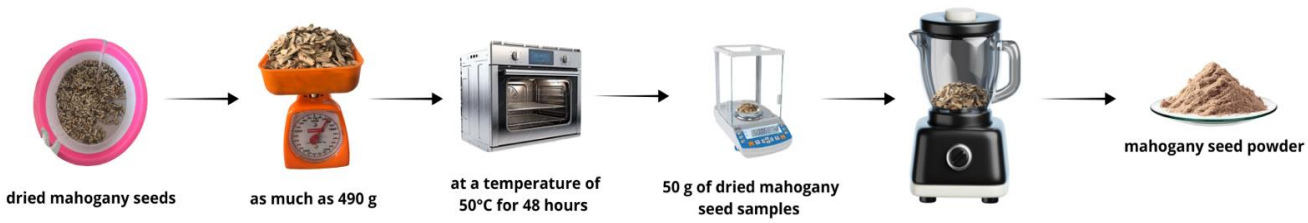

Figure 1. The illustration of sample preparation

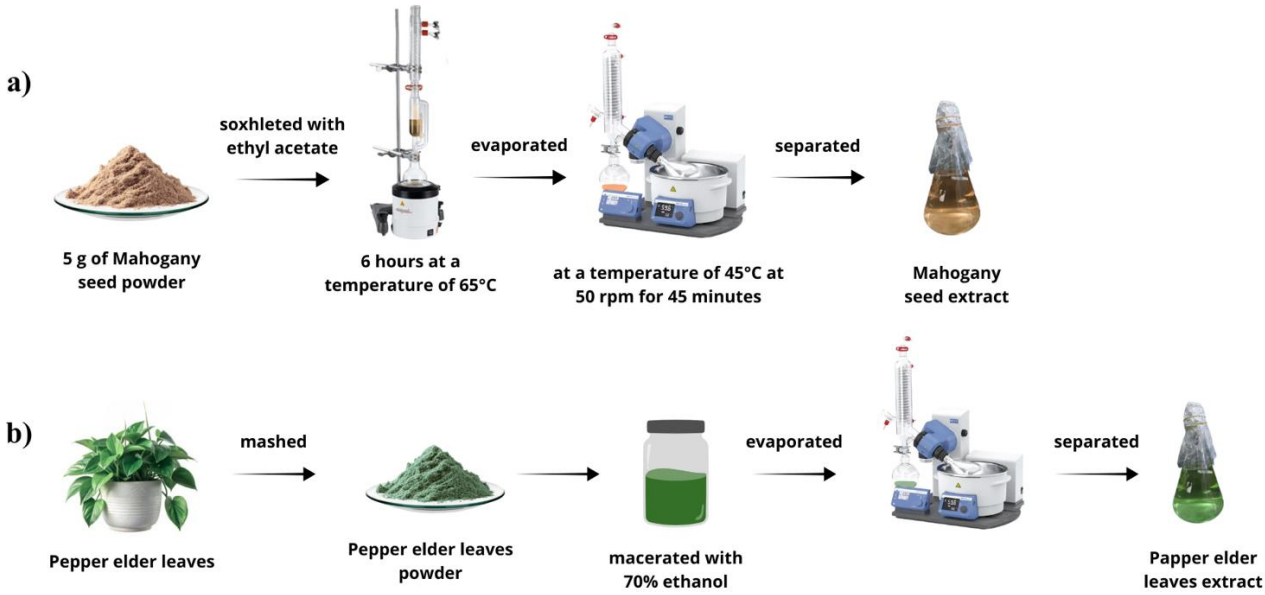

Figure 2. The illustration extraction process of (a) mahogany seeds, (b) pepper elder leaves

2.2 Formulation screening of SNEDDS

The SNEDDS preconcentrate of *Swietenia mahagoni* seed extract was prepared by combining the extract with Tween 80 as the surfactant and PEG 400 as the co-surfactant at a fixed weight ratio of 1:7:1, respectively. The components were mixed thoroughly until a clear and homogeneous isotropic system was obtained. Subsequently, the mahogany SNEDDS preconcentrate was combined with *Peperomia pellucida* leaf SNEDDS at a fixed volume of 1 mL and screened at three different volume ratios, namely 1:1, 1:2, and 2:1 (mahogany SNEDDS: pepper elder SNEDDS). The resulting mixtures were gently vortexed to ensure homogeneity and visually observed for clarity and phase stability. Three different Peperomia pellucida SNEDDS formulations, containing extract concentrations of 75 mg/mL, 100 mg/mL, and 125 mg/mL, were used during the screening process and were designated as FA, FB, and FC, respectively. The physical appearance of the screened formulations was documented as part of the preliminary evaluation.

2.3 Determination of globule size and zeta potential

The globule size and zeta potential were assessed by diluting the SNEDDS formulations of mahogany seed extract and pepper elder leaf extract with water at a 1:25 ratio under magnetic stirring until a nanoemulsion was obtained. The resulting nanoemulsion was transferred into a cuvette and analyzed using a Particle Size Analyzer (PSA). Particle size measurements were conducted using an electrophoretic light-scattering instrument (Desa Nano C Particle Analyzer, Beckman Coulter). Additionally, a 1-g mixture of oil, surfactant, and cosurfactant was dispersed in 5 mL of deionized water prior to particle size analysis.

2.4 Stability evaluation of SNEDDS

The physical stability of the SNEDDS formulations was evaluated using a series of accelerated stress tests to assess their robustness under extreme temperature and mechanical conditions. These tests were designed to identify potential physical instability, such as phase separation, creaming, or precipitation, rather than to predict long-term storage stability.

For thermal stress evaluation, SNEDDS samples were placed in sealed glass vials and subjected to elevated temperatures ranging from 60°C to 100°C for 5 h using a laboratory oven. This test was conducted to examine the tolerance of the formulations to severe thermal stress that may occur during processing, transportation, or storage under high-temperature conditions, particularly in tropical environments. After heating, samples were allowed to equilibrate to room temperature and visually inspected for any signs of phase separation, turbidity, or precipitation.

The freeze–thaw stability was assessed using a temperature cycling protocol between 4°C and 40°C. Each cycle consisted of storage at 4°C for 24 h followed by storage at 40°C for 24 h. A total of three cycles was performed for each formulation. This test was intended to simulate temperature fluctuations that may occur during refrigerated storage and exposure to elevated ambient temperatures. After completion of the cycles, the formulations were examined visually for changes in physical appearance, including phase separation or sedimentation.

In addition, a centrifugation test was performed to evaluate the resistance of the SNEDDS formulations to gravitational stress. Approximately 2 mL of each formulation was placed in a centrifuge tube and centrifuged at 10,000 rpm for 30 min. The samples were then inspected for evidence of phase separation or instability. All stability evaluations were performed in triplicate. Formulations that remained visually homogeneous without phase separation or precipitation after the stress tests were considered physically stable under the applied accelerated conditions.

2.5 Antidiabetic activity test

Healthy male albino Wistar rats weighing 200–250 g were used in this study. The animals were obtained from an accredited animal facility and housed under standard laboratory conditions (temperature 22–25°C, relative humidity 50–60%, and a 12 h light/dark cycle) with free access to standard pellet diet and water *ad libitum*. All animals were acclimatized for 7 days prior to experimentation.

Diabetes mellitus was induced by a single intraperitoneal

injection of alloxan monohydrate (150 mg/kg body weight) dissolved in sterile normal saline. To prevent initial hypoglycemia, animals were provided with 5% glucose solution for 24 h following alloxan administration. Fasting blood glucose levels were measured 72 h post-induction, and animals with blood glucose levels exceeding 200 mg/dL were considered diabetic and included in the study. A total of 36 diabetic rats were randomly divided into six groups (n = 3 per group) as follows:

a. Group I (K^+): Positive control, treated with glibenclamide (5 mg/kg BW)
b. Group II (K^-): Negative control, treated with Na-CMC (0.5% w/v)
c. Group III (SM): Treated with SNEDDS of *Swietenia mahagoni* seed extract
d. Group IV (SSC): Treated with SNEDDS of *Peperomia pellucida* leaf extract
e. Group V (SMSC1A): Treated with combined SNEDDS of *S. mahagoni* and *P. pellucida* (1:1 ratio)
f. Group VI (SMSC1B / SMSC1C): Treated with other screened combined SNEDDS formulations as specified

All SNEDDS formulations were administered orally via gastric gavage at an equivalent extract dose of 200 mg/kg body weight, once daily for 7 consecutive days. The dose was selected based on previous reports on the antidiabetic activity of herbal SNEDDS and preliminary screening data. Normal blood glucose levels were measured on the first day (D0). Blood was taken by incising the lateral tail vein of mice using a Glucometer (Nesco). 0.5 mL of blood was centrifuged for 15 minutes (12,000 rpm). Samples, standards, and blanks were read using a UV-Vis Spectrophotometer. On the third day, fasting blood glucose levels (H3) were measured again to compare with H0. Each group of test animals received treatment for 7 days.

All experimental procedures involving animals were conducted in accordance with internationally accepted guidelines for the care and use of laboratory animals and were approved by the Animal Ethics Commission Team of Hasanuddin University Animal Hospital (Approval No. 0061/KKEH/RSHUH/EC/2025).

2.6 Molecular docking study

Protein and reference ligand preparation in YASARA software involves removing unwanted parts of the protein, ligand, and co-activator. This step typically includes deleting unnecessary components to clean the structure for further analysis, such as docking or molecular dynamics simulation. The preparation process ensures that the protein-ligand complex is ready for accurate and meaningful simulation or docking studies by removing extraneous molecules that might interfere with the results. YASARA also assigns protonation states, adds hydrogen atoms, and can optimize the system's geometry before running simulations or docking. This preparation is done at a typical physiological pH (around 7.4) to mimic biological conditions. Such careful preparation supports downstream computational tasks like docking, scoring, and RMSD calculation [9, 10].

Ligand preparation using MarvinSketch is performed by protonating the ligand at physiological pH 7.4 to adjust the ligand ionization state to match biological conditions. After protonation, the ligand is saved in .mrv file format. The next step is to perform a ligand conformation search using the "Conformers search" feature in MarvinSketch to obtain various possible ligand conformational structures. The resulting conformations are saved in .mol2 file format. Next, the ligand preparation results (.mol2 file) and protein (.mol2 file after cleaning and preparation in YASARA) are used as input in the docking process using PLANTS software. In the docking process, PLANTS searches for the ligand pose or position in the protein's active site that yields the highest score, which is then estimated as the ligand's native position in the target protein structure [11-13].

3. RESULT AND DISCUSSION

3.1 Sample extraction

This stage uses samples of mahogany seeds; the results of the sample preparation show a brown powder, with a physical appearance as shown in Figure 3.

Figure 3. The physical appearance of mahogany seed powder

The mahogany seed preparation was extracted using the Soxhlet method using ethyl acetate as a solvent for 6 hours. The extraction process was carried out in 7 cycles. The resulting macerate is shown in Figure 4. The yield was 61%, calculated from the ratio of the extract weight to the dry weight of the medicinal plant.

Figure 4. Mahogany seed macerate using ethyl acetate solvent

3.2 Formulation of SNEDDS

SNEDDS synthesis was carried out using the formula of Mahogany seed extract: surfactant (Tween80): cosurfactant (PEG400) with a ratio of 1:7:1. The resulting Mahogany seed SNEDDS was then added with 1 mL of pepper elder leaf

SNEDDS. The physical appearance of the Mahogany seed and pepper elder SNEDDS formula with a ratio of 1:1, 1:2, and 2:1 is shown in Figure 5. Three variations of pepper elder leaf NEDDS were used in the study, namely pepper elder leaf NEDDS 75 mg/mL, 100 mg/mL, and 125 mg/mL, which were labeled as FA, FB, and FC, respectively.

The results of the SNEDDS formulation of Mahogany seeds and pepper elder leaves were tested for pH measurement and emulsification speed, as shown in Table 1. The transmittance percentage produced in this study was similar to previous studies, which also used Mahogany seeds as raw material for making SNEEDS [14, 15].

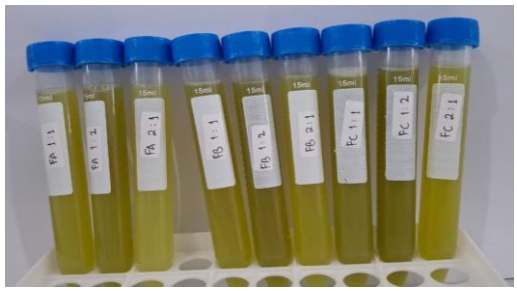

Figure 5. The physical appearance of the SNEDDS formula from mahogany seeds and pepper elder leaves with various concentrations

Table 1. The results of transmittance, pH, and emulsification rate tests of SNEDDS

Sample	Transmittance (%)	pH	Emulsification (seconds)
Blanko akuabides	110.0%	7	
SNEED Mahoni	81.5%	4.75	22.47
FA 1:1	89.0%	4.70	5.41
FA 1:2	89.1%	4.70	5.36
FA 2:1	89.1%	4.77	6.68
FB 1:1	80.9%	4.89	7.58
FB 1:2	89.4%	4.89	11.25
FB 2:1	89.7%	4.85	8.29
FC 1:1	86.9%	4.79	9.00
FC 1:2	85.7%	4.82	7.09
FC 2:1	87.9%	4.79	10.65

3.3 Characterization of SNEDDS formula of mahogany seed and pepper elder

Based on the functional group analysis using FTIR as shown in Figure 6, the spectrum of mahogany seed extract, the absorption band at 2924.09 cm^{-1} indicates the presence of –CH stretching vibrations, while the band at 2854.65 cm^{-1} corresponds to $–CH_2$ groups [16]. The absorption observed at 1373.32 cm^{-1} is attributed to the $–CH_3$ group [8]. Furthermore, the absorption peak at 1712.79 cm^{-1} confirms the presence of a C=O ester functional group, which is further supported by a broad absorption at 3464.15 cm^{-1}. Additional absorption bands at 1581.63 cm^{-1} and 1458.18 cm^{-1} suggest the existence of aromatic ring structures [14]. These spectral features collectively indicate that mahogany seed oil likely contains ester compounds with aromatic characteristics. A similar trend has been reported in earlier studies involving the extraction of mahogany leaves collected from different geographical regions and countries [17-19].

Furthermore, an amide (1580 cm^{-1}) and aromatic aliphatic C–H bonds (2937.3 and 2854.0 cm^{-1}) [20, 21], 2843.9 cm^{-1} (NCH_2), and 1489 cm^{-1} (aromatic C=C) are detected in the FTIR analysis of pepper elder leaf extract. Comparison of the individual FTIR spectra of mahogany seeds and pepper elder leaves with that of their mixture reveals several notable spectral changes, indicating intermolecular interactions and changes in the local environments of functional groups. First, the intensities and/or positions of the O–H and C=O related bands are altered in the formulation spectrum relative to the pure components: attenuation or broadening of the O–H band and slight shifts of the carbonyl band are consistent with hydrogen-bond formation between phenolic hydroxyls of the leaf extract and the ester carbonyls of the seed oil. Such hydrogen-bonding interactions commonly result in band broadening and frequency shifts and indicate a non-covalent association in the blended system [8, 14].

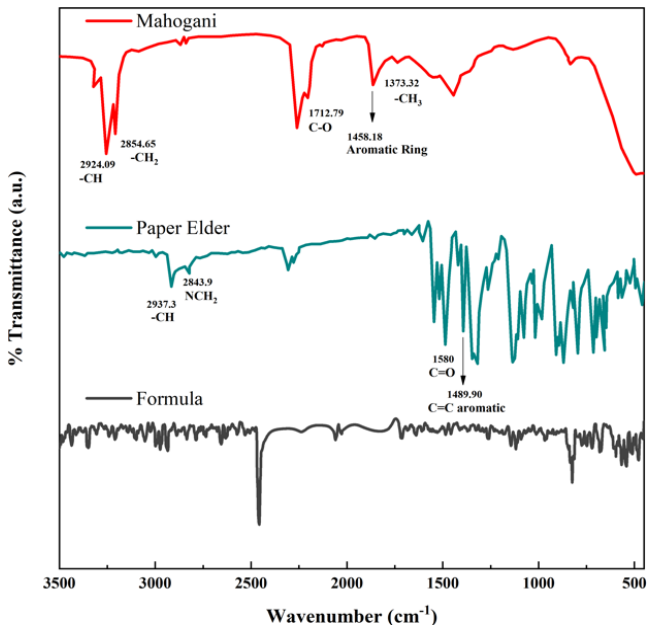

Figure 6. FTIR spectrum of mahogany seeds extract, pepper elder leaves extract, and the formula of mahogany seeds and pepper elder leaves

Second, the aliphatic C–H stretching region (2950–2850 cm^{-1}) remains evident in the mixed spectrum, confirming that the long-chain hydrocarbon framework of the seed oil persists after blending. However, changes in relative band intensities in the fingerprint region (1600–1400 cm^{-1}), namely, modulation of aromatic C=C bands, suggest that phenolic/aromatic constituents from the leaf extract interact with or are solubilized within the oil phase [22]. These spectral modifications imply the formation of a stable dispersion or complex between polar phenolics and nonpolar lipid phases rather than chemical transformation under the blending

conditions used.

The FTIR results, which revealed the presence of functional groups such as esters, aliphatic chains, and aromatic compounds, were further supported by GC–MS analysis that identified specific chemical constituents corresponding to these functional groups, as shown in Figure 7 with interpretation in Table 2. The GC-MS analysis of the SNEDDS formula revealed the presence of four major fatty acid methyl ester components: 9-octadecenoic acid (methyl oleate), hexadecanoic acid (methyl palmitate), methyl stearate, and 9,12-octadecadienoic acid (methyl linoleate). The predominance of methyl oleate indicates that the oil phase within the SNEDDS system is rich in oleic acid (C18:1), originating from both the carrier oil and the natural extracts of the plants.

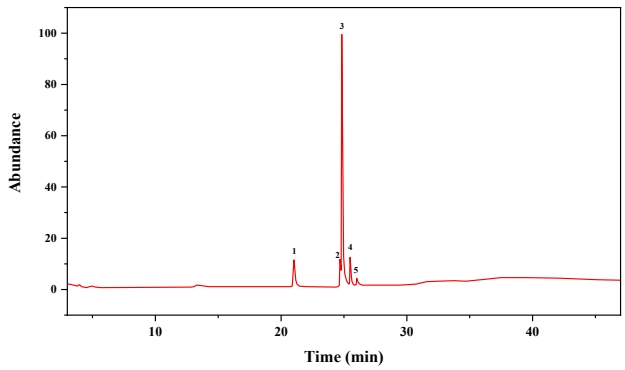

Figure 7. The GC-MS of the SNEDDS formula of mahogany seeds and pepper elder leaves

The GC-MS profile is consistent with previous studies reporting that the oil or non-polar fractions of *S. mahagoni* and *P. pellucida* contain unsaturated fatty acids such as oleate, linoleate, and palmitate [23, 24]. These fatty acids play an essential role in forming stable nanoemulsion systems and enhancing the solubility and bioavailability of lipophilic bioactive compounds such as swietenin, swietemahonin, pellucidin, and amide alkaloids, which have been reported to exhibit antidiabetic and antioxidant activities [23].

Table 2. The compound content in the SNEDDS formula, as a result of GC-MS analysis interpretation from Figure 7

Peak	Name	%Area
1	Hexadecanoic acid	8.07
2 & 5	9,12-octadecadienoic acid	6.48
3	9-octadecenoic acid, methyl ester (CAS)	61.17
4	Methyl stearate	6.20

The dominance of oleic acid (61.17%) in this formulation has significant biological implications for antidiabetic activity. Oleic acid (C18:1), a monounsaturated fatty acid (MUFA), has been demonstrated to improve insulin sensitivity and reduce insulin resistance [25]. Mechanistically, oleic acid activates the PI3K/Akt and AMPK signaling pathways, thereby promoting glucose transport into muscle and hepatic tissues [25]. Additionally, oleic acid supplementation can suppress the expression of pro-inflammatory cytokines (TNF-α and IL-6), mitigating systemic inflammation that contributes to the pathogenesis of type 2 diabetes mellitus [26].

Recent studies have shown that SNEDDS formulations can enhance the bioavailability of lipophilic antidiabetic compounds by 2–3 fold compared to conventional extract forms [27, 28]. In this context, oleic acid acts not only as an oil-phase component but also as a natural cosurfactant that reinforces nano-phase formation. These findings highlight the potential of the SNEDDS formulation containing *S. mahagoni* and *P. pellucida* extracts to enhance glucose-lowering efficacy through two primary mechanisms, namely improved absorption of lipophilic antidiabetic compounds and direct biological contribution of unsaturated fatty acids within the oil phase.

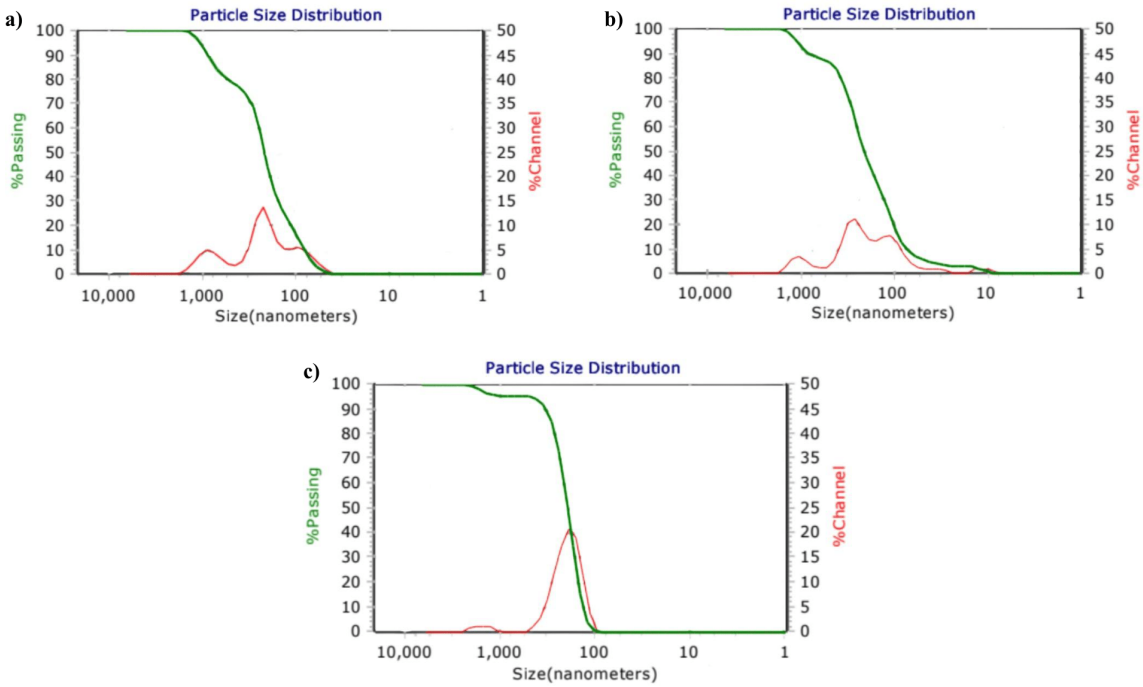

Figure 8. The distribution of globule size with variations in the ratio of mahogany leaves and pepper elder leaves, 75 mg/mL (FA) (a) 1:1, (b) 1:2, and (c) 2:1

The next characterization is the determination of globule size and zeta potential. It was carried out to predict and control the physical stability of SNEDDS with optimal globule size to avoid phase separation, zeta potential value to see the occurrence of aggregation and flocculation of particles from the resulting SNEDDS formula. Determination of globule size and zeta potential was carried out using a Particle Size Analyzer (PSA) with four repetitions. The results obtained are shown in Figures 8-10, with the results of the interpretation of globule size shown in Table 3 and the zeta potential value in Table 4.

The droplet or globule size in nanoemulsions generally ranges from 10 to 200 nanometers (nm). The interpretation of the average globule size data for the SNEDDS formula using PSA, shown in Table 3, indicates that all samples had globule sizes in the range of 1-200 nm. Furthermore, the zeta potential value in a nanoemulsion can be classified as high if the zeta potential of a particle is very positive (> +30 mV) or very negative (< -30 mV). The zeta potential is low if the zeta potential approaches zero (between -10 mV and +10 mV), resulting in weak repulsive forces.

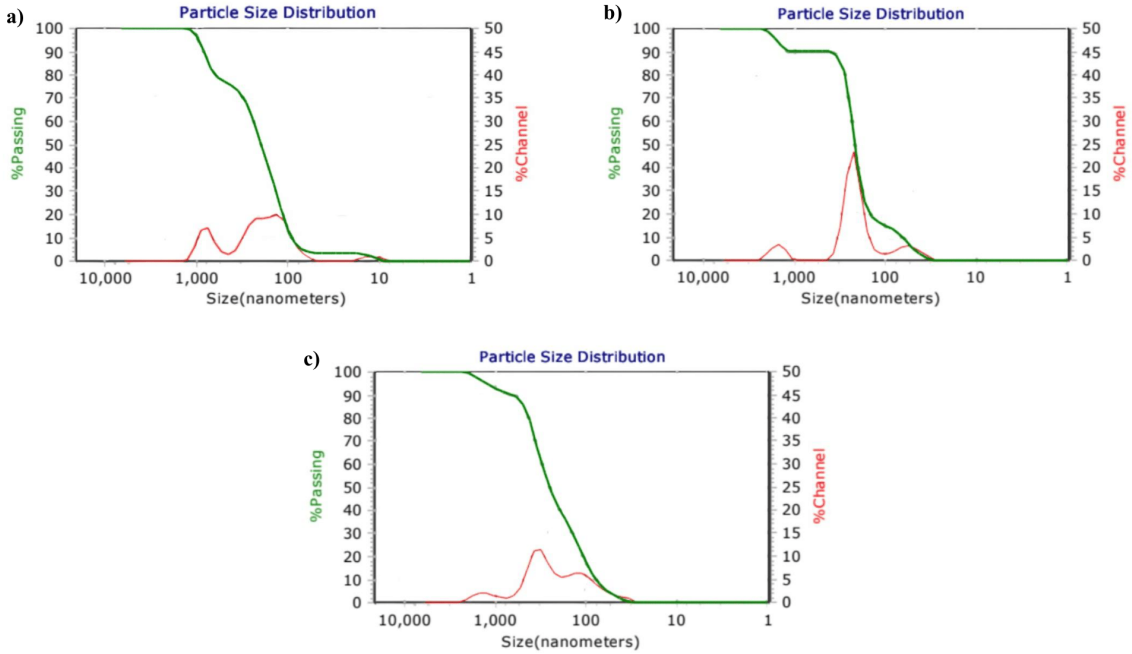

Figure 9. The distribution of globule size with variations in the ratio of mahogany leaves and pepper elder leaves, 100 mg/mL (FB) (a) 1:1, (b) 1:2, and (c) 2:1

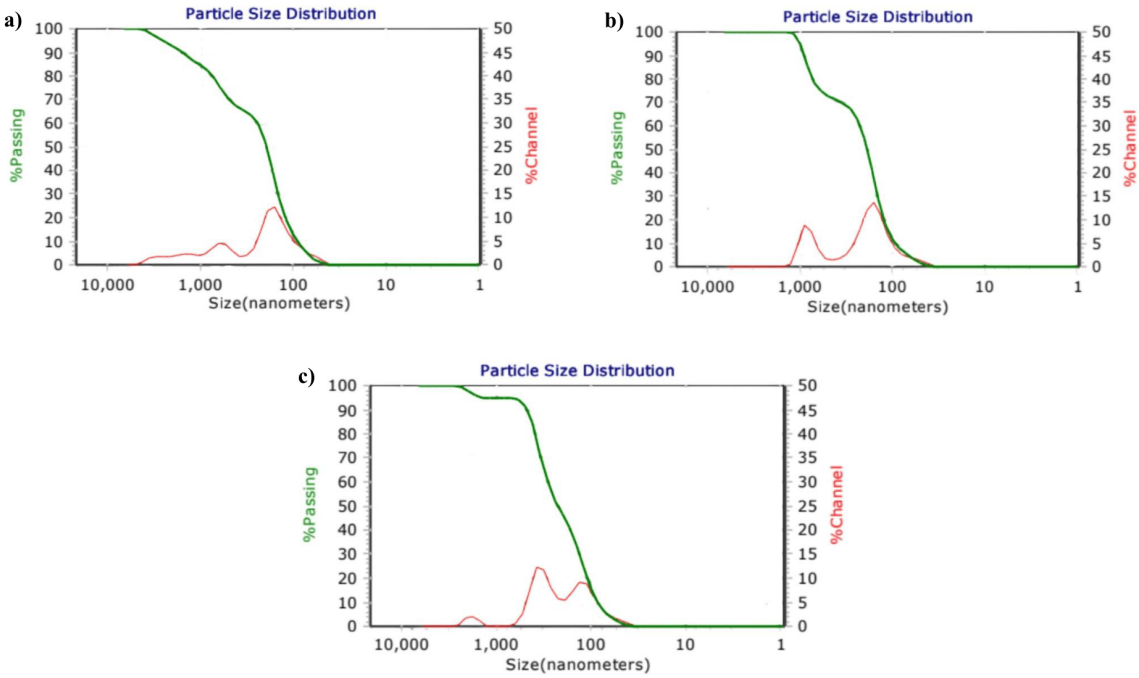

Figure 10. The distribution of globule size with variations in the ratio of mahogany leaves and pepper elder leaves, 125 mg/mL (FC) (a) 1:1, (b) 1:2, and (c) 2:1

Table 3. Results of SNEDDS globule size analysis of mahogany and *Peperomia pellucida*

Sample	Globule Size (nm)			The Average Globule Size
	1	2	3	
SNEDDS Mahony	10.89	9.73	11.43	10.68 ± 0.86
FA 1:1	77.90	74.30	100.80	117.67 ± 1.43
FA 1:2	11.51	10.87	10.34	10.91 ± 0.58
FA 2:1	191.5	204.20	192.40	196.03 ± 1.78
FB 1:1	12.21	11.23	10.45	11.29 ± 0.88
FB 1:2	105.50	187.30	157.30	133.37 ± 0.96
FB 2:1	12.28	65.10	12.30	29.89 ± 1.98
FC 1:1	150.90	151.40	143.90	148.73 ± 0.94
FC 1:2	155.30	163.50	160.60	159.80 ± 0.84
FC 2:1	112.10	221.60	117.00	150.23 ± 1.85

Table 4. Results of SNEDDS zeta potential analysis of mahogany and pepper elder

Sample	Zeta Potential (mV)			The Average of Zeta Potential
	1	2	3	
SNEED Mahoni	0.2	0.2	0.3	0.233 ± 0.05
FA 1:1	47.4	51.2	48.1	48.9 ± 1.22
FA 1:2	12.3	10.3	11.6	11.4 ± 1.01
FA 2:1	10.2	10.0	9.9	10.03 ± 0.15
FB 1:1	9.1	8.6	10.0	9.23 ± 0.71
FB 1:2	10.6	9.5	10.5	10.2 ± 0.61
FB 2:1	6.6	5.0	4.6	5.4 ± 1.05
FC 1:1	5.4	2.9	2.9	3.73 ± 1.44
FC 1:2	4.7	3.9	2.9	3.83 ± 0.90
FC 2:1	0.2	0.2	0.2	0.2 ± 0.01

Table 5. Results of SNEDDS polydispersity index (PDI) analysis of mahogany seeds and pepper elder leaves

Sample	PDI			Average PDI	Transmission (%)
	1	2	3		
SNEED Mahoni	0.539	0.958	0.663	0.72 ± 0.22	81.5
FA 1:1	0.761	1.116	0.731	0.87 ± 0.21	89.0
FA 1:2	0.420	0.608	0.371	0.47 ± 0.12	89.1
FA 2:1	0.0670	0.157	0.169	0.13 ± 0.05	89.1
FB 1:1	0.661	0.088	0.287	0.35 ± 0.29	80.9
FB 1:2	0.1579	0.077	0.211	0.15 ± 0.06	89.4
FB 2:1	0.442	0.275	0.254	0.32 ± 0.10	89.7
FC 1:1	0.575	0.598	0.567	0.58 ± 0.01	86.9
FC 1:2	0.929	0.690	0.700	0.77 ± 0.16	85.7
FC 2:1	0.2259	0.242	0.295	0.25 ± 0.03	87.9

Based on Table 3, the smallest average globule size occurred in the FB 1:1 sample of 11.29 ± 0.88 nm. The average globule size produced in this study was larger than that of previous studies that produced SNEDDS formulations from mahogany seeds [14] and SNEDDS formulations combined with mahogany seeds and moringa leaves [15]. All formulated samples met the nanoemulsion size, but the FA 2:1 sample had a very large size, namely 196.03 ± 1.78 nm. It is thought to be due to an agglomeration process, so that the desired distribution of the formula by forming small oil droplets in water (o/w) is difficult to occur [29]. The same phenomenon was also found in the SNEDDS formula, a mixture of moringa leaves and mahogany seeds [15]. Sample FB 1:1 was selected for further characterization based on formulation screening criteria, including the smallest globule size, acceptable PDI, and physical stability.

The zeta potential generated in this study (Table 4) indicates a good stability of the SNEDDS formula. A zeta potential value below 30 mV indicates a reasonably strong negative charge, and a potential value above 30 mV was only found in the FA 1:1 sample, indicating a strong positive charge. Thus, the NEDDS samples produced in this study are quite stable, safe, in line with the absorption targets, and stable in storage [3-5].

The particle size distribution within a sample is described by the PDI value in a nanoemulsion, especially when it comes to polymers or nanoparticles. Particle size variation (polydispersity) is indicated by a PDI value greater than 0. The sample's particle size variation increases with the PDI value. To determine the homogeneity of the globule size distribution of SNEDDS, the PDI measurements were conducted, as shown in Table 5, along with the transmittance percentage values. Based on Table 5, all samples of the SNEDDS formulation exhibited a homogenous globule size distribution. The results obtained are similar to previous studies that used cyproterone acetate-based SNEDDS [30]. The transmittance percentage obtained for all samples was greater than 80%, indicating a clear emulsion, which suggests that all formulas have very good biological activity. The transmittance percentage obtained is similar to previous research that used black cumin oil extract for NEDDS formulation [27]. Thus,

the SNEDDS formula from mahogani seeds and pepper elder leaves has the potential to act as an anti-diabetic.

Several previous studies reported the average droplet size in SNEDDS formulated from piperine in the range of 51-701 nm with a zeta potential between -10.6 mV and -36.4 mV [31]. Furthermore, a study reported that SNEDDS from ripe *Momordica Charantia* fruit with a size of 31.89 nm and a zeta potential of -15.65 mV had promising antidiabetic potential based on biochemical, hematological, and histopathological results in streptozotocin-induced diabetic rats [6]. In this study, the average droplet size values with the smallest size of each variation of the SNEDDS formula of mahogany seeds and pepper betel leaves ranged between 10.91 and 29.89 nm, indicating a relatively lower average droplet size.

In comparison to previously reported SNEDDS, the zeta potential of SNEDDS was found to be -0.20 to -48.9 mV, indicating improved adsorption and oxidative stability of the formulation. Additionally, the study's zeta potential generally showed that droplet coalescence is prevented by an increase in electrostatic repulsion between nanoemulsion droplets. On the other hand, phase separation would result from a reduction in electrostatic repulsion. The homogeneity of the nanoemulsion particles is shown by the PDI value. The PDI value ranged from 0.13 to 0.87, with the value of 0.13 increasing with particle homogeneity. It demonstrates the effectiveness of SNEEDS as a solvent and for medication absorption.

3.4 Test for antidiabetic activity

The antidiabetic activity test was conducted using Wistar albino rats in an in vivo study. The results of the antidiabetic activity test are shown in Table 6. Values are expressed as mean ± standard deviation (SD). Different superscript letters indicate statistically significant differences between treatment groups ($p < 0.05$), as determined by one-way ANOVA followed by an appropriate post hoc test. This study investigated the antidiabetic effects of several treatment formulations (SM, SSC, SMSC1A, SMSC1B, and SMSC1C) in diabetic-induced animal models, using changes in blood glucose levels as the main pharmacodynamic parameter.

The results showed clear differences in glucose-lowering efficacy across treatment groups, as reflected in both absolute reduction and percentage reduction values.

Table 6. Results of SNEDDS antidiabetes activity analysis of mahogany seeds and pepper elder leaves

Treatment	Blood Sugar (mg/dL)			Level of Blood Sugar Decrease After Treatment (mg/dL) (P1-P2)	Percentage of Decrease in Blood Sugar Levels (%)
	P0 (initial sugar level)	P1 (alloxan)	P2 (after treatment)		
K+	136.00	142.00	125.00	17.00	0.15±9.71[a]
K-	127.67	139.33	170.00	-30.67	-0.29±13.0[a]
SM	106.67	141.33	104.00	37.33	0.08±5.80[b]
SSC	99.00	140.67	103.00	37.67	0.54±3.05[b]
SMSC1A	105.67	167.33	122.67	44.67	0.40±6.64[b]
SMSC1B	119.33	143.67	122.33	21.33	0.18±6.52[a]
SMSC1C	134.00	140.33	113.67	26.67	0.13±0.78[b]

where, K+ = Glibenclamide; K- = Sodium carboxymethyl cellulose (NaCMC); SM = SNEDDS Mahogany; SSC = NEDDS Pepper elder; SMSC1A = SNEDDS FB (1:1); SMSC1B = SNEDDS FB (1:2); SMSC1C = SNEDDS FB (2:1); P0 = Initial blood sugar levels before alloxan induction; P1 = Blood sugar levels after alloxan induction; P2 = Blood sugar levels after treatment.

The negative control (K^-) group exhibited an increase in blood glucose levels, with an average change of –45 units, confirming that hyperglycemia was successfully induced and maintained in the absence of intervention. In contrast, the positive control (K^+) group showed a reduction of 17 units (~5.50%), consistent with the expected effect of a standard antidiabetic agent, thereby validating the experimental model [32]. The formula of the SSC (37.67 mg/dL and SM (37.33 mg/dL) groups also showed promising activity, although with higher variability between subjects.

Among all samples, the formula of SMSC1A demonstrated the highest hypoglycemic activity, with a mean reduction of 44.67 units and percentage reductions ranging from 17% to 82%. This finding is relevant because a reduction of ≥30% in blood glucose in rodent models is generally classified as a pharmacologically significant antidiabetic effect [33]. The extreme difference observed in some animals, 142.85% reduction in SSC, indicates strong individual variability, which is commonly reported in chemically induced diabetic models such as Streptozotocin (STZ) and Alloxan [34]. Such variability may result from differences in β-cell destruction, metabolic rate, tissue insulin sensitivity, or differential response to phytochemical constituents.

The observed glucose-lowering effect is consistent with prior studies reporting that plant-derived bioactive compounds, particularly flavonoids, alkaloids, terpenoids, and phenolics, may reduce blood glucose through multiple mechanisms, including pancreatic β-cell regeneration, α-glucosidase inhibition, AMPK activation, insulin sensitization, and enhancement of glucose transporter (GLUT-4) expression [35]. Similar antidiabetic profiles have also been demonstrated in extracts of *Muntingia calaburaand* Hibiscus species, which decreased blood glucose by 40–60% in rodent models [36, 37].

However, the present study has several limitations. The sample size per group (n = 3) was relatively small, resulting in high variability and limited statistical power. Additionally, no biochemical markers such as insulin, HbA1c, lipid profile, or oxidative stress enzymes were measured, which restricts mechanistic interpretation. Future studies should include histopathological analysis of pancreatic tissue, dose–response testing, and molecular pathway evaluation to validate the pharmacological mechanism [8].

Overall, the findings indicate that SMSC1A and SSC are promising candidates for further development as antidiabetic agents, with higher efficacy compared to the positive control. Nevertheless, confirmatory studies with expanded sample size, controlled dosing, and additional biomarkers are required before they can be considered for preclinical formulation or phytopharmaceutical development.

3.5 Molecular docking of 9-octadecenoic acid with protein tyrosine phosphatase

The RMSD between the docking result and its reference compound was 2.1877 Å. The RMSD value approaching 2 Å indicates that the protocol can be used to accurately generate poses resulting from interactions between ligands and proteins [38]. It indicates the success of the protocol in replicating the crystal conformation of the ligand in the protein's active site, a common validation criterion in molecular docking studies [39]. In general, RMSD values below 2 Å are often considered a successful indicator of predicting biologically relevant ligand binding positions. However, it is important to note that RMSD alone does not necessarily reflect all aspects of molecular interactions, and values higher than 2 Å can also provide valid conformations, especially when accompanied by stable binding energy analysis or without significant steric interference [40].

A molecular docking study was conducted to evaluate the binding interaction of 9-octadecenoic acid, the major bioactive compound identified through GC–MS analysis of SNEDDS formula from mahogany seeds and pepper elder leaves, with the protein tyrosine phosphatase 1B (PDB ID: 5KQG). This enzyme is known to play a crucial role in the pathogenesis of diabetes mellitus. Biologically, PTP functions as a negative regulator of the insulin signaling pathway through dephosphorylation of the insulin receptor and its substrate (IRS), leading to decreased insulin sensitivity [41]. Overexpression or hyperactivity of PTPs, particularly PTP1B, has been strongly associated with insulin resistance, one of the hallmarks of type 2 diabetes mellitus. Therefore, molecules capable of binding to and inhibiting PTP activity may enhance insulin signaling and exert antidiabetic effects.

The docking performance was validated using a reference inhibitor 2-(benzothiazol-2-ylamino)-2-oxo-1-phenylethanesulfonic acid, which has been reported to interact with the same protein target [38]. Validation of the docking protocol was achieved by redocking the control ligand into the active site of PTP, yielding an RMSD value of 2.1877 Å between the experimental and predicted poses (Figure 11). This value falls within the acceptable range (RMSD < 2.5 Å), confirming that the docking method accurately reproduces ligand orientation and binding conformation. The validation result ensures the reliability of subsequent interaction analyses.

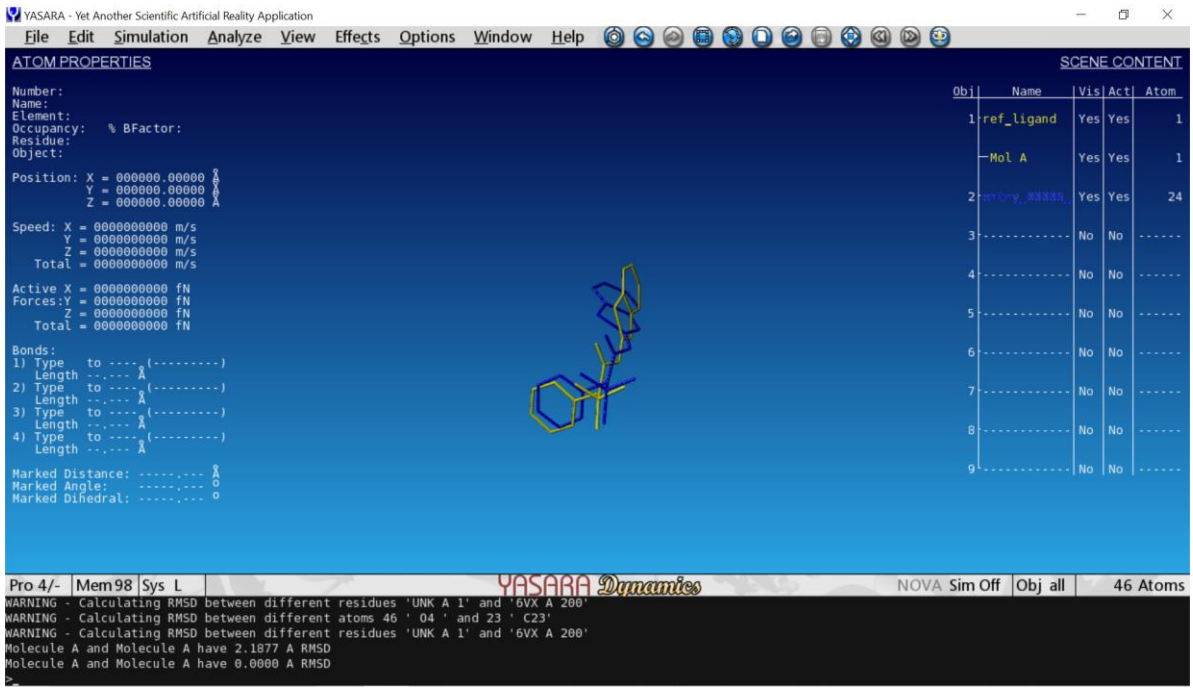

Figure 11. Overlapping pose of the reference compound obtained from the structure of the control compound 2-(benzothiazol-2-ylamino)-2-oxo-1-phenylethanesulfonic acid (carbon atoms in yellow) and the pose of the docked compound (carbon atoms in blue)

Docking results revealed that 9-octadecenoic acid exhibited a binding energy of –100.14 kcal/mol, while the control compound displayed a slightly lower energy value of –112.75 kcal/mol, indicating a stronger affinity. Although the control ligand demonstrated a more stable complex, the binding energy of 9-octadecenoic acid still reflects a stable and biologically relevant interaction with the enzyme's active site. This finding suggests that 9-octadecenoic acid has the potential to modulate the activity of PTP, thereby influencing glucose homeostasis.

Visualization of the interaction between 9-octadecenoic acid and the amino acid residues of PTP (Figure 12) revealed predominant hydrophobic alkyl and π–alkyl interactions with residues LEU116, ILE127, CYS145, CYS148, VAL8, VAL41, and PHE410 (represented by light purple lines). Additionally, van der Waals interactions (light green lines) were observed with GLU23, SER19, VAL11, ALA44, and LEU89, suggesting weak attractive forces between nonpolar moieties of the ligand and the side chains of the protein. A single carbon–hydrogen bond (C–H···O) was also identified between the carbonyl group of the ligand and residue PHE152. The combination of these nonpolar interactions indicates that 9-octadecenoic acid binds stably within the active pocket of 5KQG, primarily through hydrophobic and van der Waals forces.

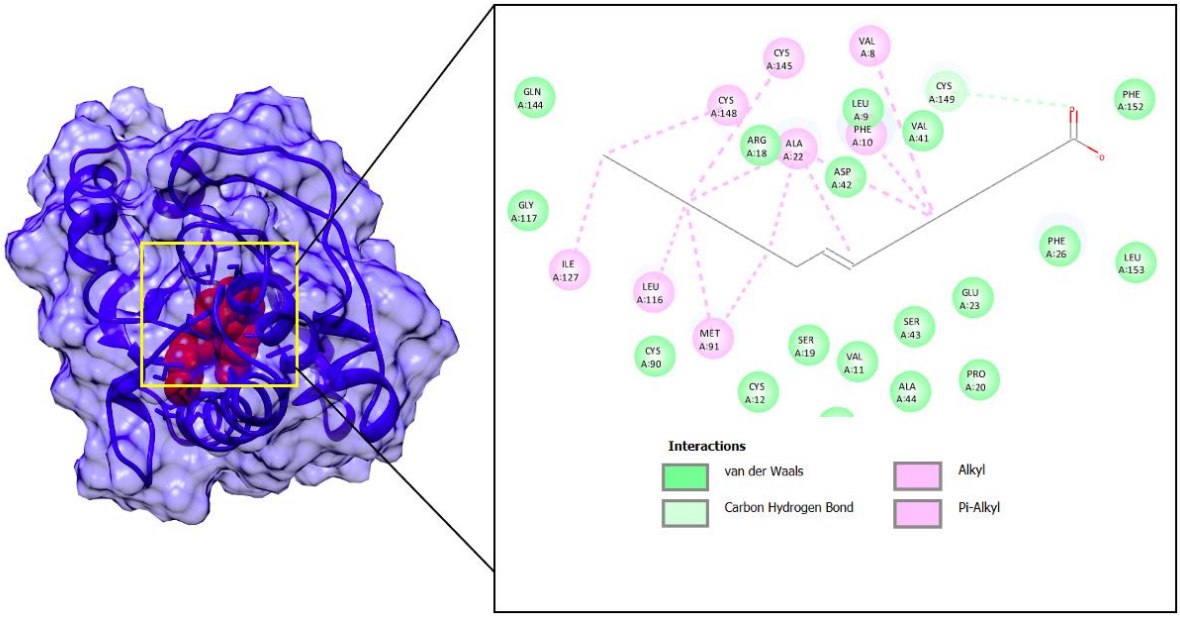

Figure 12. Visualization of the interaction between 9-octadecenoic acid and the amino acid residues of protein tyrosine phosphatase (5KQG)

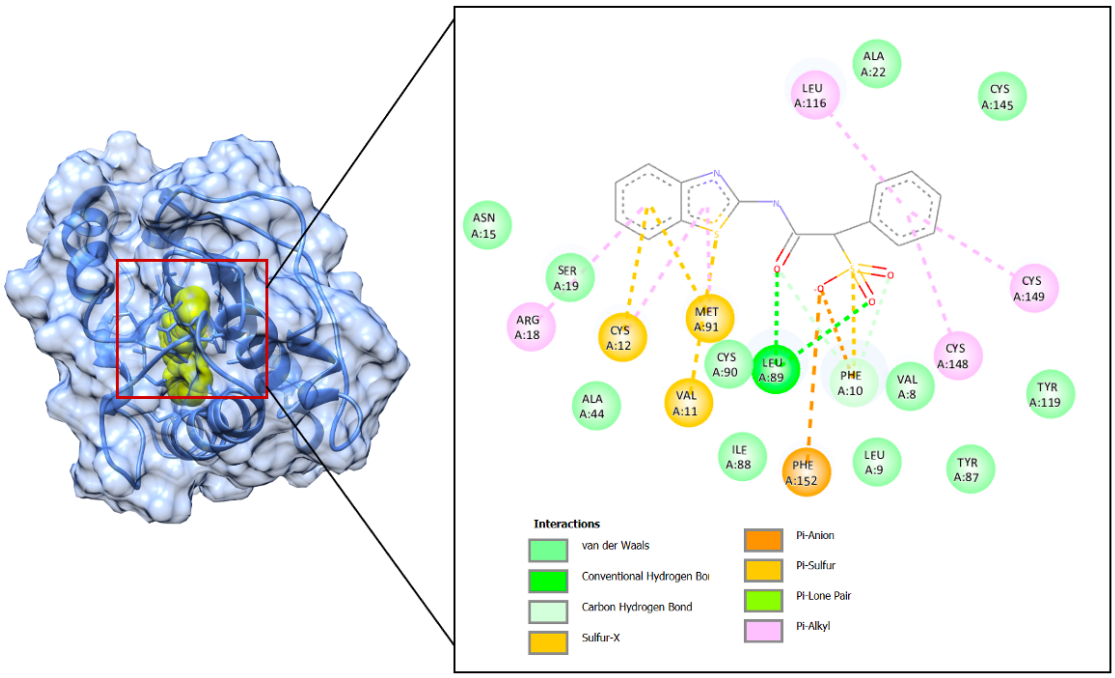

Figure 13. Visualization of the interaction between the control compound 2-(benzothiazol-2-ylamino)-2-oxo-1-phenylethanesulfonic acid and the amino acid residues of protein tyrosine phosphatase (5KQG)

In contrast, visualization of the control ligand 2-(benzothiazol-2-ylamino)-2-oxo-1-phenylethanesulfonic acid interactions with PTP residues (Figure 13) demonstrated a more complex and robust binding pattern. Conventional hydrogen bonds were formed with residue LEU89 (light green line), representing a strong electrostatic attraction between the ligand's polar groups and the protein's amide groups. Additional sulfur–X and π–sulfur interactions with residues CYS12, MET91, and PHE152 (yellow/orange lines) highlighted the contribution of sulfur atoms from the benzothiazole ring to complex stabilization. A π–anion interaction with residue PHE152 was also detected, indicating electrostatic attraction between the aromatic ring of the ligand and a negatively charged residue. Furthermore, π–alkyl interactions (light purple lines) with residues CYS148, LEU116, and CYS149, along with van der Waals interactions (light green lines) involving ALA44, SER19, VAL8, and TYR87, further enhanced the stability of the ligand–receptor complex. This combination of diverse interactions explains the lower (more stable) binding energy observed for the control ligand.

A comparative analysis between the two ligands showed that the control compound possessed stronger binding affinity and more complex interaction networks with PTP than 9-octadecenoic acid, as reflected in both binding energy and interaction profile. Nevertheless, the substantial hydrophobic interactions exhibited by 9-octadecenoic acid suggest that this fatty acid still holds potential as a natural inhibitor candidate

for PTP.

Overall, the docking results support the hypothesis that unsaturated fatty acids derived from *S. mahagoni* and *P. pellucida* contribute to the previously reported antidiabetic activity of these plants. The findings provide mechanistic insight into the potential role of 9-octadecenoic acid in modulating PTP activity and enhancing insulin sensitivity.

It should be noted that GC–MS detects fatty acids predominantly in their methyl ester forms, whereas molecular docking was performed using the corresponding free fatty acid, which may exhibit different interaction profiles. Therefore, the docking results should be interpreted as providing mechanistic support rather than definitive evidence of the biological activity of the methyl ester identified.

4. CONCLUSIONS

The study demonstrated that the SNEDDS containing a combination of *Swietenia mahagoni* and *Peperomia pellucida* extracts possesses excellent physicochemical properties and significant antidiabetic potential. The predominance of oleic acid (9-octadecenoic acid) in the GC–MS profile, supported by molecular docking results against PTP1B, confirms its potential as a bioactive compound capable of enhancing insulin sensitivity and regulating glucose homeostasis. The nanoscale droplet size, favorable zeta potential, and low PDI values indicate that the developed SNEDDS is physically stable and capable of improving the bioavailability of lipophilic phytoconstituents. These findings provide a scientific basis for further in vivo pharmacokinetic and toxicological studies to validate the clinical applicability of the *S. mahagoni* and *P. pellucida* SNEDDS formulation as a promising natural therapeutic strategy for diabetes mellitus.

ACKNOWLEDGMENT

We would like to express our gratitude for the financial support provided by the Directorate of Research and Community Service, Ministry of Education, Culture, Research, and Technology, through research grant Number: 084/C3/DT.05.00/PL/2025; 2902/UN36.11/TU/2025 with decree Number: 0419/C3/DT.05.00/2025.

REFERENCES

[1] Fardous, J., Omoso, Y., Joshi, A., Yoshida, K., Patwary, M.K.A., Ono, F., Ijima, H. (2021). Development and characterization of gel-in-water nanoemulsion as a novel drug delivery system. Materials Science and Engineering: C, 124: 112076. https://doi.org/10.1016/j.msec.2021.112076

[2] Khursheed, R., Singh, S.K., Kumar, B., Wadhwa, S., et al. (2022). Self-nanoemulsifying composition containing curcumin, quercetin, Ganoderma lucidum extract powder and probiotics for effective treatment of type 2 diabetes mellitus in streptozotocin induced rats. International Journal of Pharmaceutics, 612: 121306. https://doi.org/10.1016/j.ijpharm.2021.121306

[3] Putri, S.E., Ahmad, A., Raya, I., Tjahjanto, R.T., Irfandi, R. (2023). Synthesis and antibacterial activity of chitosan nanoparticles from black tiger shrimp shell (Penaeus monodon). Egyptian Journal of Chemistry, 66(8): 129-139. https://doi.org/10.21608/ejchem.2022.148340.6417

[4] Tanuku, S., Velisila, D., Thatraju, D., kumar Vadaga, A. (2024). Nanoemulsion formulation strategies for enhanced drug delivery. Journal of Pharma Insights and Research, 2(4): 125-138. https://doi.org/10.69613/3f8m9151

[5] Wilson, R.J., Li, Y., Yang, G., Zhao, C.X. (2022). Nanoemulsions for drug delivery. Particuology, 64: 85-97. https://doi.org/10.1016/j.partic.2021.05.009

[6] Garg, V., Kaur, P., Singh, S.K., Kumar, B., Bawa, P., Gulati, M., Yadav, A.K. (2017). Solid self-nanoemulsifying drug delivery systems for oral delivery of polypeptide-k: formulation, optimization, in-vitro and in-vivo antidiabetic evaluation. European Journal of Pharmaceutical Sciences, 109: 297-315. https://doi.org/10.1016/j.ejps.2017.08.022

[7] Garg, V., Kaur, P., Gulati, M., Singh, S.K., et al. (2019). Coadministration of polypeptide-k and curcumin through solid self-nanoemulsifying drug delivery system for better therapeutic effect against diabetes mellitus: Formulation, optimization, biopharmaceutical characterization, and pharmacodynamic assessment. Assay and Drug Development Technologies, 17(4): 201-221. https://doi.org/10.1089/adt.2018.902

[8] Sukardiman, Ervina, M. (2020). The recent use of Swietenia mahagoni (L.) Jacq. as antidiabetes type 2 phytomedicine: A systematic review. Heliyon, 6(3): e03536. https://doi.org/10.1016/j.heliyon.2020.e03536

[9] Pratiwi, E., Raya, I., Natsir, H., Irfandi, R., et al. (2024). Investigations of Ni (ii) cysteine-tyrosine dithiocarbamate complex: Synthesis, characterization, molecular docking, molecular dynamic, and anticancer activity on MCF-7 breast cancer cell line. Asian Pacific Journal of Cancer Prevention: APJCP, 25(4): 1301-1313. https://doi.org/10.31557/APJCP.2024.25.4.1301

[10] Arfah, R.A., Pratiwi, E., Raya, I., Natsir, H., et al. (2024). Design, synthesis and characterization of Mn (II) cysteine-tyrosine dithiocarbamate complex for against the cancer on MCF-7 breast cancer cell line. Asian Pacific Journal of Cancer Prevention: APJCP, 25(9): 3251-3261. https://doi.org/10.31557/APJCP.2024.25.9.3251

[11] Raya, I., Kartina, D., Wijaya, R.I., Irfandi, R., et al. (2023). Novel complex of Zinc (II) dichloroethylenediamine: Synthesis, characterization, In-silico, and In-vitro evaluation against cervical cancer cells. Asian Pacific journal of cancer prevention: APJCP, 24(12): 4155-4165. https://doi.org/10.31557/APJCP.2023.24.12.4155

[12] Irfandi R, Raya I, Ahmad A, Fudholi A, Riswandi, Santi S, et al. (2024). Design anticancer potential of Zn(II)isoleucinedithiocarbamate complex on MCF-7 cell lines: Synthesis, characterization, molecular docking, molecular dynamic, ADMET, and in-vitro studies. Mol Divers, 28: 3199-3214. https://doi.org/10.1007/s11030-023-10747-y

[13] Irfandi, R., Raya, I., Ahmad, A., Fudholi, A., Putri, S.E., Jarre, S., Sari, D.R.T. (2024). Evaluation of anticancer and anticovid potential of Zn (II) prolinedithiocarbamate complex: Molecular docking simulation. AIP Conference Proceedings, 2774(1): 030012. https://doi.org/10.1063/5.0164491

[14] Taiyeb, M., Hartati, H., Arwansyah, A., Muis, A.,

Mu'nisa, A., Arif, A.R., Salleh, L.M. (2024). Self-Nanoemulsifying Drug Delivery System (SNEDDS) formulation and molecular docking of mahogany seed extract (Swietenia mahagoni) as anti-hyperglycemic. Informatics in Medicine Unlocked, 47: 101517. https://doi.org/10.1016/j.imu.2024.101517

[15] Hartati, H., Hartono, H., Karim, H., Putri, S.E., Sahribulan, S., Kusdianawati, K., Negara, S.P.J. (2025). Self-Nanoemulsifying Drug Delivery System (SNEDDS) for antidiabetic formulation from mahogany seeds (Swietenia Mahagoni Jacq) and Moringa oleifera. International Journal of Design & Nature and Ecodynamics, 20(2): 373-381. https://doi.org/10.18280/ijdne.200214

[16] Mursiti, S., Rahayu, E.F., Rosanti, Y.M., Nurjaya, I. (2019). Mahogany seeds oil: Isolation and characterizations. IOP Conference Series: Materials Science and Engineering, 509(1): 012137. https://doi.org/10.1088/1757-899X/509/1/012137

[17] Hossain, M., Goni, L.K.M.O., Muntaha, N., Jamal, M.S., et al. (2021). Box–Behnken design-based optimization for biodiesel production from waste cooking oil using Mahogany (Swietenia macrophylla) fruit shell derived activated carbon as a heterogeneous base catalyst. Reaction Kinetics, Mechanisms and Catalysis, 133(1): 117-138. https://doi.org/10.1007/s11144-021-01995-w

[18] Razzaq, M.A., Rahman, M.M., Rahman, M.M., Ullah, M.S. (2024). Sky Fruit Seed Crush (SFSC): A Potential Source of less Salt Curing of Raw Goatskin. Journal of the American Leather Chemists Association, 119(6): 247-254.

[19] Nuriana, W., Winarni, M., Arfan, N.A., Fudholi, A. (2023). Coloring of mahogany (Swietenia macrophylla King.) on textiles with mordant process and fixation against fastness. International Journal of Design & Nature and Ecodynamics, 18(5): 1097-1102. https://doi.org/10.18280/ijdne.180510

[20] Wulandari, C., Iswandaru, D., Mora, A.M., Anggraini, D., Dessy, A., Novriyanti. (2025). Ethnomedical practices and medicinal plant use in Tanjung and Seponjen Villages, Jambi, Indonesia. International Journal of Design & Nature and Ecodynamics, 20(2): 419-428. https://doi.org/10.18280/ijdne.200219

[21] Aziz, D.M., Hama, J.R., Alam, S.M. (2015). Synthesising a novel derivatives of piperine from black pepper (Piper nigrum L.). Journal of Food Measurement and Characterization, 9(3): 324-331. https://doi.org/10.1007/s11694-015-9239-2

[22] Mursiti, S. (2017). Isolation and antimicrobial activity of flavonoid compounds from mahagony seeds (Swietenia macrophylla, King). IOP Conference Series: Materials Science and Engineering, 172(1): 012055. https://doi.org/10.1088/1757-899X/172/1/012055

[23] Ojha, P.K., Poudel, D.K., Rokaya, A., Maharjan, S., et al. (2024). Chemical compositions and essential fatty acid analysis of selected vegetable oils and fats. Compounds, 4(1): 37-70. https://doi.org/10.3390/compounds4010003

[24] Tuan, C.T., Men, T.T. (2024). Peperomia pellucida's ingredients, antioxidant properties, and safe usage as food and herbal medicine. Journal of Microbiology and Biotechnology, 34(11): 2321. https://doi.org/10.4014/jmb.2406.06025

[25] Vari, F., Bisconti, E., Serra, I., Stanca, E., Friuli, M., Vergara, D., Giudetti, A.M. (2025). Exploring the Role of Oleic Acid in Muscle Cell Differentiation: Mechanisms and Implications for Myogenesis and Metabolic Regulation in C2C12 Myoblasts. Biomedicines, 13(7): 1568. https://doi.org/10.3390/biomedicines13071568

[26] Silveira, E.A., Rosa, L.P.D.S., de Resende, D.P., Rodrigues, A.P.D.S., et al. (2022). Positive effects of extra-virgin olive oil supplementation and DietBra on inflammation and glycemic profiles in adults with type 2 diabetes and class II/III obesity: A randomized clinical trial. Frontiers in Endocrinology, 13: 841971. https://doi.org/10.3389/fendo.2022.841971

[27] Priani, S.E., Maulidina, S.S., Darusman, F., Purwanti, L., Mulyanti, D. (2020). Development of self nanoemulsifying drug delivery system for black seed oil (Nigella sativa L.). Journal of Physics: Conference Series, 1469(1): 012022. https://doi.org/10.1088/1742-6596/1469/1/012022

[28] Tanga, S., Ramburrun, P., Aucamp, M. (2026). From liquid SNEDDS to solid SNEDDS: A comprehensive review of their development and pharmaceutical applications. The AAPS Journal, 28(1): 1-18. https://doi.org/10.1208/s12248-025-01167-x

[29] Salawi, A. (2022). Self-emulsifying drug delivery systems: A novel approach to deliver drugs. Drug Delivery, 29(1): 1811-1823. https://doi.org/10.1080/10717544.2022.2083724

[30] Namazi, N.I. (2025). Self Nano-Emulsifying Drug Delivery System (Snedds) for cyproterone acetate: Formulation, characterization and pharmacokinetic evaluation. Results in Chemistry, 14: 102118. https://doi.org/10.1016/j.rechem.2025.102118

[31] Kazi, M., Shahba, A.A., Alrashoud, S., Alwadei, M., Sherif, A.Y., Alanazi, F.K. (2020). Bioactive self-nanoemulsifying drug delivery systems (Bio-SNEDDS) for combined oral delivery of curcumin and piperine. Molecules, 25(7): 1703. https://doi.org/10.3390/molecules25071703

[32] Eddouks, M., Chattopadhyay, D., Zeggwagh, N.A. (2012). Animal models as tools to investigate antidiabetic and anti‐Inflammatory plants. Evidence‐based Complementary and Alternative Medicine, 2012(1): 142087. https://doi.org/10.1155/2012/142087

[33] Jethi, S., Mishra, S.K., Satapathy, K.B. (2022). Study of anti-diabetic activity of Alstonia Scholaris (L.) R. BR. root extract. International Journal of Health Sciences, 6: 9056-9066. https://doi.org/10.53730/ijhs.v6nS3.8225

[34] Kottaisamy, C.P.D., Raj, D.S., Prasanth Kumar, V., Sankaran, U. (2021). Experimental animal models for diabetes and its related complications—A review. Laboratory Animal Research, 37(1): 23. https://doi.org/10.1186/s42826-021-00101-4

[35] Trasca, D.M., Dop, D., Stoica, G.A., Adrian, N.S., Carmen, N.E., Văruț, R.M., Singer, C.E. (2025). The antidiabetic activity of wild-growing and cultivated medicinal plants used in Romania for diabetes mellitus management: A phytochemical and pharmacological review. Pharmaceuticals, 18(7): 1035. https://doi.org/10.3390/ph18071035

[36] Aligita, W., Susilawati, E., Sukmawati, I.K., Holidayanti, L., Riswanti, J. (2018). Antidiabetic activities of Muntingia calabura L. leaves water extract in type 2 diabetes mellitus animal models. The Indonesian Biomedical Journal, 10(2): 165-170.

https://doi.org/10.18585/inabj.v10i2.405
[37] Viado, A.E.E., Purnamasari, L., dela Cruz, J.F. (2022). Anti-diabetic effects of Hibiscus spp. extract in rat and mice models: A review. Jurnal Gizi Indonesia (The Indonesian Journal of Nutrition), 11(1): 39-48. https://doi.org/10.14710/jgi.11.1.39-48
[38] Kamerlin, N., Delcey, M.G., Manzetti, S., Van der Spoel, D. (2020). Toward a computational ecotoxicity assay. Journal of Chemical Information and Modeling, 60(8): 3792-3803. https://doi.org/10.1021/acs.jcim.0c00574
[39] Devaurs, D., Antunes, D.A., Hall-Swan, S., Mitchell, N., Moll, M., Lizée, G., Kavraki, L.E. (2019). Using parallelized incremental meta-docking can solve the conformational sampling issue when docking large ligands to proteins. BMC Molecular and Cell Biology, 20(1): 42. https://doi.org/10.1186/s12860-019-0225-9
[40] Ghedira, D., El Harran, A.A., Abderrazak, H. (2023). Design and study of bioisosteric analogues of the drug Molnupiravir as potential therapeutics against SARS-COV-2: An in silico approach. In Silico Pharmacology, 12(1): 1. https://doi.org/https://doi.org/10.1007/s40203-023-00171-3
[41] Islam, W.U., Khan, F., Waqas, M., Ullah, S., et al. (2023). In-vivo anti-diabetic and anti-hyperlipidemic effects of natural metabolites from resin of Commiphora mukul and their in-silico to in-vitro target fishing. Biomedicine & Pharmacotherapy, 165: 115214. https://doi.org/10.1016/j.biopha.2023.115214